Available online at www.sciencedirect.com
ScienceDirect
Journal of the European Ceramic Society 26 (2006) 3909–3917
www.elsevier.com/locate/jeurceramsoc

Corrosion of Si_3N_4-ceramics in aqueous solutions Part I: Characterisation of starting materials and corrosion in 1 N H_2SO_4

J. Schilm [a], W. Gruner [b], M. Herrmann [c,*], G. Michael [c]

[a] *Institute of materials science, Technical University of Dresden, 01062 Dresden, Germany*
[b] *Leibnitz Institute for Solid State and Materials Research, Helmholtzstrasse 20, 01069 Dresden, Germany*
[c] *Fraunhofer Institute for Ceramic Technologies and Sintered Materials (IKTS), Winterbergstrasse 28, 01277 Dresden, Germany*

Received 29 July 2005; received in revised form 24 November 2005; accepted 3 December 2005
Available online 31 January 2006

Abstract

The corrosion behaviour of silicon nitride materials in acids strongly depends on the composition and amount of the grain boundary. But there exist no systematic investigations of the relation between the corrosion behaviour and the composition and amount of the grain-boundary phase. The aim of the series of these papers is the systematic investigation of these relations. In the first part the methods of determination of the amorphous grain-boundary phases are described in detail. Additionally, the correlation between the corrosion behaviour and the composition of the grain-boundary phases are given. The structural reasons and the mechanisms behind the observed changes in the corrosion behaviour will be given in part II of this paper.

Keywords: Si_3N_4; Corrosion; Aqueous corrosion

1. Introduction

Silicon nitride materials are one of the most prominent structural ceramics and are applied in areas were high strength, fracture toughness, hardness and corrosion resistance are necessary, such as ball bearings, cutting tools and parts in heat combustion engines. Silicon nitride materials contain beside silicon nitride grains the grain boundary, formed by the sintering additives and the SiO_2, existing on the surface of the used Si_3N_4 powder. Recent investigations of the corrosion resistant of Si_3N_4 materials have shown that the corrosion rate and the corrosion mechanism strongly depend on the composition of the grain-boundary phase, especially on the SiO_2 content of the grain boundary.[1–4] Therefore, the knowledge of the composition of the grain-boundary phase is essential to the interpretation of the properties of the materials. This is the reason why part I of this series of papers on the corrosion of silicon nitride materials is focused on the determination of the composition of grain-boundary phases.

The grain-boundary phase is predetermined by the additives used for the sintering of silicon nitride. But the composition of the grain boundary is not equivalent to the concentration of the additives, which were used for preparation of the ceramics, due to several interactions during sintering:

- The SiO_2 on the surface of the starting powder reacts with the additives forming the amorphous phase. Depending on the sintering conditions SiO_2 partially decomposes during sintering forming surface gradients or even result in metallic Si inclusions in the material.[5]
- The often-used Al_2O_3 partially dissolves into the Si_3N_4 grains due to the reaction:

$$0.5zAl_2O_3 + (2 - 0.25z)Si_3N_4 \leftrightarrow Si_{6-z}Al_zN_{8-z}O_z + 0.25zSiO_2 \quad (1)$$

By TEM investigations was observed that the content of 63% Al_2O_3 in the starting grain-boundary composition reduces to only 20% Al_2O_3 in the grain-boundary phase after sintering.[6] This indicates the strong interaction of Al_2O_3 with the Si_3N_4 powder during sintering.

* Corresponding author.
E-mail address: herrmann@ikts.fhg.de (M. Herrmann).

0955-2219/$ – see front matter © 2005 Elsevier Ltd. All rights reserved.
doi:10.1016/j.jeurceramsoc.2005.12.001

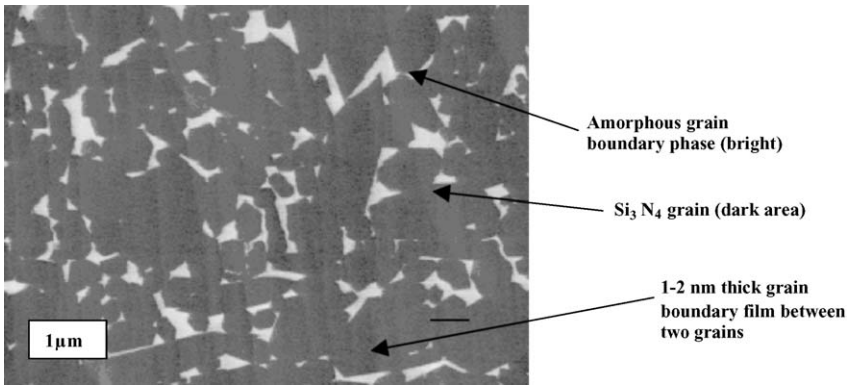

Fig. 1. FESEM-micrograph of a microstructure of a Si_3N_4 ceramic.

The grain-boundary phase consists of thin films between two grains (thickness 1–2 nm) and triple junctions in the micrometer range (Fig. 1). Recent TEM investigations have shown that the thin films can exhibit a different concentration of the elements than the triple junctions.[7] This could have an influence on the composition and crystallisation behaviour of the triple junctions.[8]

Considering an overall grains size of ≥0.3 μm and a thickness of the thin films of 1 nm, the relation between the volume of the grain-boundary phase in the thin films and in the triple junctions as a function of the overall volume content of the ceramic can be calculated (Fig. 2). The diagram shows that for materials with more than 5 vol.% grain-boundary phases the shift of the composition in the triple junction due to the effect of the different composition of the thin films could be neglected.

There exist different methods for the determination of the composition of the triple junctions of the grain-boundary phase. The first method is TEM analysis. To get consistent values a lot of triple junctions have to be analysed. Additionally, the quantitative determination of the light elements is complicated. Also the preparation of TEM specimen is a time- and cost-consuming procedure. Therefore, TEM cannot be used as a standard method for the determination of the composition of the grain boundary.[6]

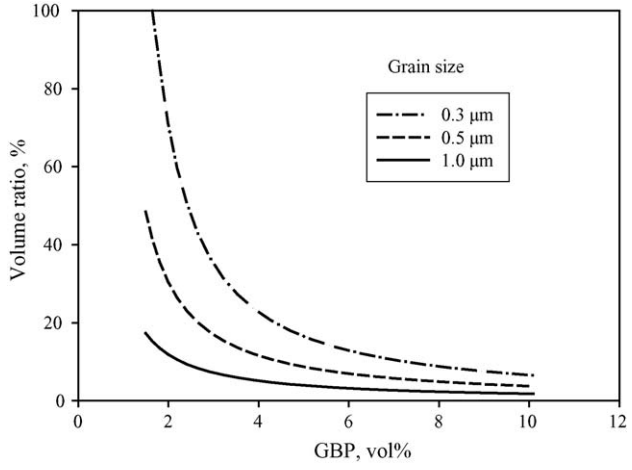

Fig. 2. Calculated ratio between the volume of the thin grain-boundary films and the overall volume content of the grain-boundary phase as a function of the volume of the grain-boundary phase (GBP) and three different mean grain sizes.

Rabe et al.[9] described a method of selective chemical dissolution of the grain-boundary phase in HF and analysing both the composition of the solution and the remaining non-dissolved grains. Especially recent corrosion experiments have shown that it is difficult to dissolve the grain-boundary phase completely without a partial dissolution of grains.[10] It is known from literature, that the amount of Al and O incorporated into silicon nitride crystal lattice as solid solution can be determined by X-ray diffraction.[1]

For Si_3N_4 powders[11] and for AlN[12] ceramics it was shown that oxygen species in the grains and at the surface can be distinguished with the temperature-controlled carbothermal reduction carried out in a commercial oxygen/nitrogen analyser.

Therefore, the aim of this article is to examine methods of determination of the composition of the grain-boundary phase by combination of oxygen analysis and X-ray diffraction. Based on these investigations, the corrosion behaviour of Si_3N_4 materials is correlated with the composition of the grain-boundary phases.

2. Experimental

2.1. Materials

Series of materials were produced from α-Si_3N_4 powder (UBE SN E 10), Al_2O_3 (AKP50), Y_2O_3 (grade fine HCST) and SiO_2 (Heraeus T125) with a systematic variation of the sintering additives (Table 1). The silicon nitride ceramics of KORSiN-type 1–9 were prepared from raw powders, which were suspended in isopropanol and mixed 4 h in an attrition mill (Fa. Getzmann). After 4 h milling, the powders were dried in a Rotavap and granulated using a 400 μm sieve. Samples of about 100 g (20 mm × 20 mm × 70 mm) were formed by cold isostatic pressing (250 MPa). The samples were gas-pressure sintered at 1825 °C to a density of >99.5% of the theoretical density. The materials SN0 and SN_3 were produced by mixing the components in an aqueous solution in an attrition mill, spray drying and subsequent cold isostatic pressing at 200 MPa into plates of 6 mm × 60 mm × 60 mm. Afterwards the organic binder was removed by heat treatment in air at 550 °C. Then the samples were sintered to full density in a gas-pressure sintering furnace at 1850 °C.

Table 1
Starting composition, density after sintering, z-values by XRD, overall oxygen and nitrogen content by CGHE method

Sample	Si_3N_4 (wt.%)	Y_2O_3 (wt.%)	Al_2O_3 (wt.%)	SiO_2 (wt.%)	Density (g cm^{-3})	z-Value	O (wt.%)	N (wt.%)
KORSiN 1	93.3	4.0	2.7	–	3.232	0.13		
KORSiN 7	91.3	4.0	2.7	2.0	3.217	0.09	4.78	34.81
KORSiN 7 leached	91.3	4.0	2.7	2.0	–	–	1.21	33.04
KORSiN 4	90.0	6.0	4.0	–	3.251	0.176	4.61	34.12
KORSiN 2a	88.5	6.0	4.0	1.5	3.242	0.157	5.61	33.52
KORSiN 8	88.0	6.0	4.0	2.0	3.236	0.145	6.01	33.46
KORSiN 9	87.5	6.0	4.0	2.5	3.230	0.141	6.21	33.28
KORSiN 9 leached	87.5	6.0	4.0	2.5	–	–	1.97	33.28
KORSiN 6	87.0	6.0	4.0	3.0	3.228	0.145	6.34	33.38
KORSiN 5	83.7	8.0	5.3	3.0	3.249	0.168	7.44	31.71
KORSiN 5 leached	83.7	8.0	5.3	3.0	–	–	1.46	35.97
SN0	90.0	6.0	4.0	–	3.245	0.149	5.25	33.81
SN3	90.0	6.0	4.0	–	3.243	0.175	5.01	34.20

The samples were cut from the inner of larger blocks, so that they do not contain any sintering skins. For the oxygen analyses the samples were crushed in a hard metal-lined vibrational mill to grain sizes smaller than 100 μm and than sieved at 40 μm. The fraction less than 40 μm was used for the oxygen analysis. The powders were dried and stored in a dry nitrogen atmosphere. Additionally, for some materials the grain-boundary phase was leached out of crushed samples with a mixture of 0.5 mol/l H_2SO_4 and 17 mmol/l KF at 40 °C for 72 h. This was done to get an independent value of the oxygen content of the Si_3N_4 grains.

2.2. Methods of analysis

2.2.1. Oxygen analysis

The oxygen content of the starting powder mixtures, the sintered samples, and the special prepared samples (leaching) was measured by the carrier gas hot extraction method (CGHE) with the oxygen/nitrogen analyser TC436-DR (LECO). Two IR-selective detectors registered simultaneously the formed reaction species CO and CO_2, whose amounts are correlated to the oxygen content in the sample. For total oxygen determination the powders (about 25 mg) were encapsulated in Ni/Sn. This pressed package was dropped into a degassed high-temperature graphite crucible, which was electrically heated with a power (temperature)–time program. For the analysis of the distribution of the oxygen the samples were mixed 1:1 with spectral pure graphite. The mixture was placed directly into graphite crucibles and heated continuously in the dynamic ramping mode from 1000 to 3000 W heating power within 400 s or in the two-step isothermal mode where firstly the mixture is heated in a power (temperature)-controlled mode over 400 s, and secondly the resulting product is analysed under the same conditions as for total analysis. Important, the oxygen signal and the signal of nitride decomposition were always registered simultaneously. All measurements were repeated three times at minimum. The typical reproducibility is about 1% relative standard deviation (R.S.D.) for the total oxygen determination and about 0.5% R.S.D. for the nitrogen ones. The calibration of the analyser has been carried out with reference materials in different measurement modes.

2.2.2. X-ray diffraction

The amorphous state of the grain-boundary phases of the Si_3N_4-ceramics and the lattice parameter of β-Si_3N_4 were determined by XRD. These values were used for the calculation of the z-values of β-$Si_{(6-z)}Al_zO_zN_{(8-z)}$ grains by $a = 0.7603 + 0.002967z$ and $c = 0.2907 + 0.002554z$, were a and c are the lattice parameters.[1,13]

The z-value is directly connected with the amount of Al incorporated into the β-Si_3N_4-grains. For the measurements, the diffractometer XRD7 (Seifert-FPM) with Cu Kα-radiation, step size 0.02 degree between 20° and 90° and a counting time 10 s were used. High-purity Si ($a = 0.543088$ nm) was used as internal standard for the determination of the lattice constants. For checking the results, pure β-Si_3N_4-powder was produced by sintering a Si_3N_4 raw powder with Yb_2O_3 and also analysed by the same method. The z-value determined for this powder was 0.01 ± 0.01 indicating the accuracy of the method.

2.3. Corrosion experiments

All corrosion tests were carried out in a 1.5l teflon reaction vessel equipped with teflon sample holders in 1 N H_2SO_4, i.e. 0.5 M H_2SO_4. The test samples were plates with dimensions 16 mm × 16 mm × 2.5 mm. The ratio between the surface of the samples and the volume of the acid was lower than 0.005 m^{-1}. The solutions were continuously stirred and completely changed after 15–25 h to avoid a strong enrichment of dissolved glass components. A thermostat filled with silicone oil was used to heat the vessel. The requested temperature was maintained within a range of ±0.5 K.

The standard preparation procedure before and after all corrosion experiments was to wash the samples in acetone for 10 min, rinse them with deionised water, drying for ≥2 h at 150 °C and to weigh them on a microbalance ($\Delta m = 0.01$ mg) after a 2-h cooling period.

Cross-sections of the corroded samples were investigated by optical and scanning electron microscopy. Corrosion indicators, like the thickness of corroded layers, were evaluated by quantitative image analysis (Image Tool v3). The chemical composition across the corrosion layers were analysed by SEM Stereoscan

S 260 attached with EDX detector. Therefore, the samples were coated with carbon.

3. Results and discussion

3.1. Oxygen analysis

The results of the determination of the total oxygen and nitrogen contents are listed in Table 1. The O/N content of the Si_3N_4 powder itself was determined as 1.17% O and 38.58% N, respectively. The oxygen values of the materials are a little bit higher than the expected ones from the stoichiometric calculation of mixtures of the used oxides additives and Si_3N_4 powder. This may be caused by the hydrolysis of Si_3N_4 during milling of the raw powders. The chemical leaching of KORSiN 5, 7, and 9 results in desired decreasing of grain-boundary phase content and as a consequence in a reduction of the oxygen content. In the samples KORSiN 7 and 9 the leaching process was not complete, as will be shown below.

The principle shape of the curves of oxygen release during dynamic oxide reduction analysis is demonstrated in Figs. 3 and 4. During dynamical heating of the mixture of the sample with carbon, both signals from oxygen species and nitrogen were simultaneously recorded. Three maxima in the oxygen signal curve were measured. The first one (O-I) correlates with blank and contamination effects of the powders. The third large oxygen release O-III coincides with the nitrogen detection. According to the interpretation of Kitayama,[11] this signal implies that it corresponds to the oxygen content dissolved in the Si_3N_4-grains. The same interpretation of simultaneous detection of oxygen and nitrogen species was given by Thomas[12] for AlN powder too. The equivalent second oxygen release O-II should result from the oxynitride grain-boundary phase if this phase reacts at temperatures below the nitride decomposition. Kitayama[11] applied for the peak fit a Gaussian distribution algorithm. The physico-chemical background, however, is a kinetic effect depending on measurement parameters as the heating rate, the gas flow conditions of carrier gas inside the analyser, etc. The peak profile used in our procedure is derived from the nitrogen

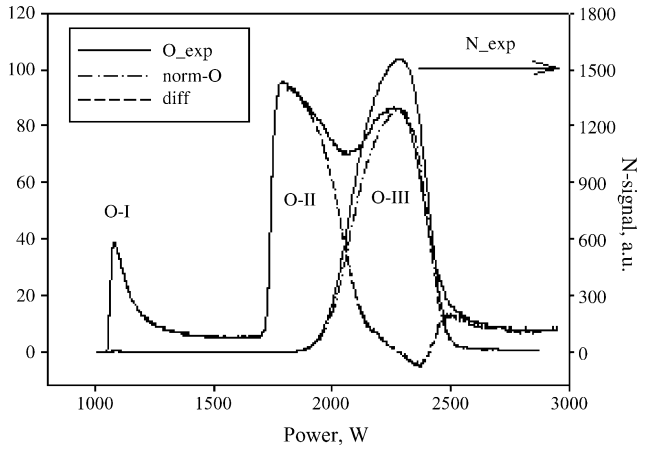

Fig. 3. Carbothermal reduction by dynamical heating (measurement curves and principle of deconvolution) at Si_3N_4 powder UBE SNE10.

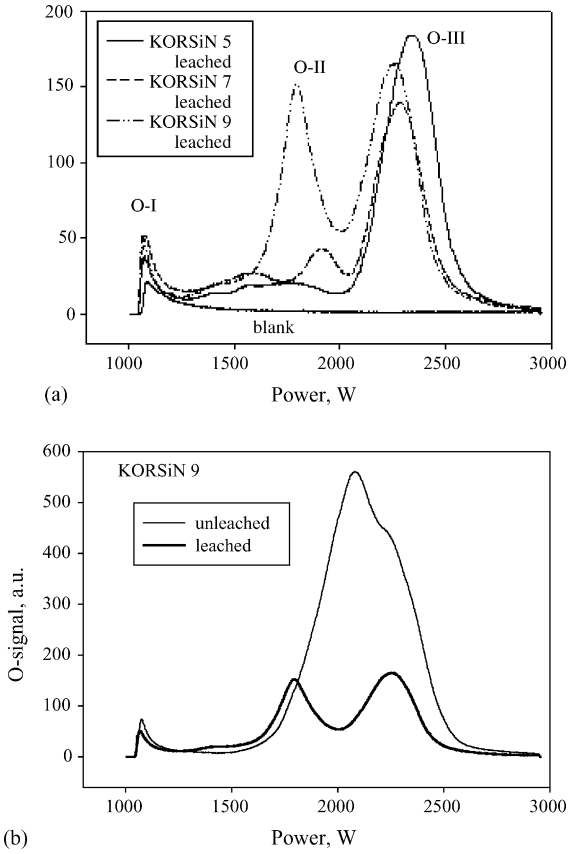

Fig. 4. Carbothermal reduction by dynamical heating (a) of partially leached samples and (b) of KORSiN 9 in the unleached and leached state.

detection curve, which is coupled with the reaction of oxygen in the Si_3N_4 grains. This shape of the nitrogen curve is normalized to the oxygen curve ('norm-0'), which is interpreted as O-III part and subtracted from the experimental oxygen curve (Fig. 3). The resulting difference curve ('diff') without the first part O-I up to about 1300 W is used for calculation of O-II and assumed to be attributed to the grain-boundary phase.

The analysis of leached samples is suitable for proving this assumption. As seen in Fig. 4a the leaching was not completed in KORSIN 7 and especially in KORSIN 9. The influence of surface oxide due to the crushing of the samples can be neglected due to the low specific surface area. The oxygen content related to part II (O-II) is measured with an acceptable reproducibility in the leached samples (Table 2).

The amount of the overall oxygen content determined by dynamic analysis is less than the amount measured by the standard method (see Yield-O% in Table 2). In the same time the yield of nitrogen content (Yield-N%) is nearly 100% for the leached samples and about 95% for the other materials. The relative good reproducibility of the nitrogen signal indicates that under these conditions the samples are nearly completely decomposed. The most probable reason for the lower determined oxygen content is that due to the use of an 'open' reaction system with flowing carrier gas some of the oxygen could not be detected (e.g. condensed as SiO or Al_2O at colder parts of the equipment). Therefore, the relative amount of oxygen in part O-II and O-III was normalized on the total oxygen content determined by the

Table 2
Quantitative results of oxygen species analysis ($n = 3$) by dynamic method

Sample	Via oxygen species determination				Value via z-value:
	Yield-O (%)	Yield-N (%)	O-II (wt.%)	O-III (wt.%)	O-lattice (wt.%)[a]
UBE SNE10	107	100	0.58	0.51	–
KORSiN 7	89	97	3.54	1.24	0.76
KORSiN 7 leached	74	99	0.36	0.84	0.87
KORSiN 9	84	94	4.80	1.41	0.67
KORSiN 9 leached	76	99	0.96	1.01	0.84
KORSiN 5	90	93	5.30	2.14	0.76
KORSiN 5 leached	75	98	0.25	1.21	0.96
SN0	85	95	3.86	1.39	0.73

Yield-0, oxygen content determined by dynamic method/divided by oxygen content determined by standard method; Yield-N, nitrogen content determined by dynamic method/divided by nitrogen content determined by standard method.
[a] Oxygen dissolved in the $Si_{6-z}Al_zN_{8-z}O_z$ lattice.

standard method. A good agreement was observed between the data determined for the SiAlON-grains in the leached samples and the data determined by XRD using the z-values (Table 2). Using the same procedure for the determination of different kinds of oxygen from the non-leached materials, it is obviously that a large overlapping in the region of O-II and O-III takes place as it is demonstrated for KORSiN 9 (Fig. 4b). The determined amount of oxygen in O-III is nearly two times higher than in the leached samples (Table 2). The results indicate that a quantitative distinction between the oxygen in the grain boundary and the oxygen dissolved in the grains is not certain by this dynamical reduction method for large glassy phase contents.

Thomas[12] has developed a different method for the determination of the oxygen distribution in AlN ceramics. He applied a two-step procedure for the investigation of the oxygen species. He stopped the dynamic heating at such a power where the nitrogen starts to evolve. The resulting product was then analysed by the total oxygen method. We modified this approach. With respect to the situation of large oxide contents in sintered samples, we preferred an isothermal reduction step where the oxygen species which reacts before nitride decomposition was determined quantitatively (O-iso) in combination with the subsequent product analysis (O-prod).

The power (temperature) for isothermal reduction was changed between 1600 and 2200 W.

Under the given conditions no sharp transition exists between the reduction of oxygen species adhered to the grain-boundary phase and oxygen species adhered to the Si_3N_4 grains. Also under these conditions no clear separation between the oxygen in the grain boundary and the oxygen dissolved in the Si_3N_4 lattice could be achieved.

In general, with both methods (dynamical and isothermal reduction) the oxygen concentrations in the Si_3N_4 grains are over estimated with respect to the oxygen dissolved in Si_3N_4 grains of the starting material and calculated using XRD data (Table 2). The strong overlapping effect due to large grain-boundary phase contents hampers the sharp differentiation between glassy phase and the Si_3N_4 phase.

The reasons for the insufficient distinction between oxide incorporated in the Si_3N_4 grains and the grain-boundary phase are caused by the structure and chemistry. The analysed particles

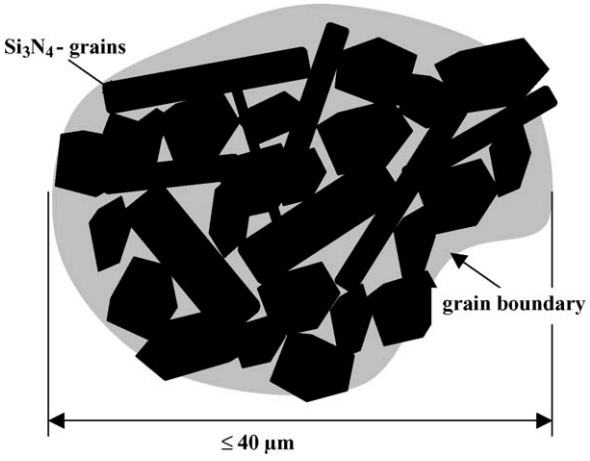

Fig. 5. Schematic view of the structure of the analysed particles.

with the grain size of ≤40 μm consist of Si_3N_4 grains embedded in the grain-boundary phase as schematically shown in Fig. 5.

The oxide glassy phase is reduced carbothermally starting from the surface. The completeness of the reaction is determined by the rate of penetration into the centre of the particles. The reaction is temperature dependent for different oxide compositions of glassy phase. For these reasons the thermodynamic and kinetic criteria for a distinction between the grain-boundary phase and the Si_3N_4 grains is not exactly defined. Besides other simultaneous reactions can take place, as that of the interaction of grain-boundary phase with the Si_3N_4 grains.

$$Si_3N_4 + 3SiO_2\,(\text{grainboundary}) \Rightarrow 6SiO\uparrow + 2N_2\uparrow \quad (2)$$

or different decomposition reactions of the Si_3N_4-grains

$$Si_3N_4 + 3C \Rightarrow 3SiC + 2N_2\uparrow \quad (3)$$

$$Si_3N_4 \Rightarrow 3Si + 2N_2\uparrow \quad (4)$$

Pure Si_3N_4 powders, which have normally grain sizes less than 5 μm and materials with lower oxide additives as the leached powders can be analysed by the dynamic and isothermal oxygen determination methods to quantify the amount of oxygen in the grains and on the surface of the powder.

3.2. Composition of the grain-boundary phase

The determination of the composition of the grain boundary is based on the results of the XRD analysis and on the total oxygen content determined by the hot-gas extraction method because any attempts to separate the oxygen incorporated into the grains by hot-gas extraction method were not successful.

The incorporation of Al and O into the β-Si_3N_4 grains can be controlled by determination of the lattice parameter and calculating the z-value of β-$Si_{(6-z)}Al_zO_zN_{(8-z)}$.[1] The results of the measurements are given in Table 1. Using the determined total oxygen content of the sintered Si_3N_4 ceramics the composition of the oxide components of the grain boundary can be calculated using the following assumptions:

- all Y_2O_3 remains in the grain boundary
- Al_2O_3 which is not incorporated into the grains is solved in the grain boundaries $Al_2O_{3,gb}$
- the SiO_2 content of the grain boundary can be calculated from the total oxygen content. From this value the O dissolved in the lattice ($O_{lattice}$) and connected with Al_2O_3 and Y_2O_3 ($O_{Al_2O_3}$ and $O_{Y_2O_3}$) has to be subtracted.

$$\text{wt.\%}(SiO_2) = \frac{60}{32}(O_{total} - O_{lattice} - O_{Al_2O_{3,gb}} - O_{Y_2O_3}) \quad (5)$$

- The SiO_2 is dissolved in the grain boundary.

An uncertain parameter is the amount of Si_3N_4 dissolved in the grain-boundary phase. Spectroscopic measurements of oxynitride glasses reveal that nearly all nitrogen atoms in YSiAlON-glasses with compositions of interest are connected to silicon atoms and have network building properties.[14–17] The grain-boundary phase is amorphous. The determined oxygen compositions are inside the glass-forming regions with a nitrogen content of 10–16 eq.% nitrogen. Own XRD measurements of oxynitride glasses with similar compositions as the grain-boundary phase reveal a maximal nitrogen content of 7 mol% or ≈16.5 eq.% dissolved in the glass.[18] The maximum solubility of silicon nitride was determined by the weight content of the crystalline Si_3N_4 in the investigated samples. Based on these results the solubility of Si_3N_4 in the grain boundary was considered as constant with an amount of 17 eq.% N. These results allow the calculation of the compositions of the grain-boundary phases, which are given in Table 3. In Fig. 6 the calculated Al_2O_3/Y_2O_3 ratios are shown as a function of the amount of the grain-boundary phase. The data show the strong difference of the composition of the grain boundary in comparison to the starting composition. The Y_2O_3/Al_2O_3 ratio in the grain boundary decreases systematically with increasing additive content.

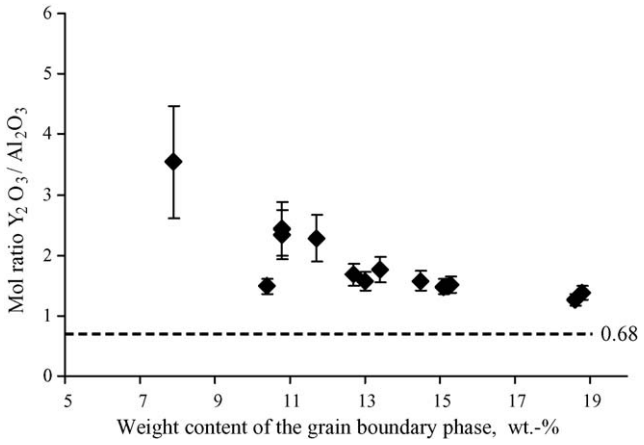

Fig. 6. Change of the mol ratio of Al_2O_3/Y_2O_3 in the grain boundary as a function of the content of the grain-boundary phase (Al_2O_3/Y_2O_3-ratio in the starting additives was 0.68).

The grain-boundary phases are amorphous. Therefore, the structure can be described in the same manner as for glasses. From glass science it is known, that the structure of the network and the properties of glasses can be described by the number of bridging anions (X) per network forming cation M.[14,16,19] The network is formed by MX_4-tetrahedra containing silica and alumina as cations. Alumina is only to a certain extent as a network-forming component incorporated into the glass network. The remaining fraction of aluminium forms five- or six-fold coordinated polyhedrons, which act as network modifiers.

Table 3
Compositions of the Si_3N_4 materials and the calculated grain boundary phases after sintering calculated from the oxygen distributions in the sintered ceramics

Material	Compositions of the raw materials				Compositions of the grain-boundary phases					
	Si_3N_4 (wt.%)	Y_2O_3 (wt.%)	Al_2O_3 (wt.%)	SiO_2 (wt.%)	Total amount (wt.%)	SiO_2 (wt.%)	Al_2O_3 (wt.%)	Y_2O_3 (wt.%)	Si_3N_4 (wt.%)[a]	X
KORSiN 1	93.3	4.0	2.7	–	7.2	29.4	7.0	55.2	8.4	2.02
KORSiN 4	90.0	6.0	4.0	–	10.6	25.5	10.9	56.6	7.0	1.38
KORSiN 2a	88.5	6.0	4.0	1.5	12.8	32.5	12.2	46.8	8.5	2.45
KORSiN 8	88.0	6.0	4.0	2.0	13.6	34.2	12.8	44.2	8.8	2.68
KORSiN 5	83.4	8.0	5.3	3.0	17.8	30.2	16.0	44.8	9.0	2.57
KORSiN 6	87.0	6.0	4.0	3.0	14.8	38.0	12.3	40.6	9.1	2.80
KORSiN 9	87.5	6.0	4.0	2.5	14.3	36.0	13.0	42.1	9.0	2.76
KORSiN 7	91.3	4.0	2.7	2.0	9.9	47.5	2.5	40.2	9.7	2.80
SN0	90.0	6.0	4.00	–	11.1	24.3	13.9	54.1	7.7	2.26
SN3	90.0	6.0	4.00	–	10.6	25.5	10.2	56.7	7.6	1.90

X, number of bridging anions per network forming tetrahedron.
[a] Assumed as 17 eq.% N.

Other components such as yttrium, magnesium or calcium are considered as network modifiers, which produce non-bridging oxygen atoms.

Risbud[16] expanded this model to describe the viscosity of alumina containing oxynitride glasses. He calculated the numbers of bridging anions:

$$X = 8 - 2\frac{[O] + [N]}{[Si] + 0.66[Al]} \quad (6)$$

[O], [N], [Si] and [Al] are concentrations in atom%.

His model indicates that in oxynitride glasses approximately two-third of aluminium cations are located in network forming tetrahedrons. This formula also implies that nitrogen takes part in the formation of the network. It does not take into account that one nitrogen forms three bonds and therefore, three bridges between three tetrahedra as for example in the Si_3N_4 crystal structure.[1] Including this fact the number of bridging anions (X) per network forming cation can be described by:

$$X = 8 - 2\frac{[O] + 1.5[N]}{[Si] + 0.66[Al]} \quad (7)$$

The X values calculated on this equation for the compositions of the grain-boundary phases are given in Table 3. For Illustration, the parameter X for a glass consisting of 100% SiO_2 or 100% Si_3N_4 has a value of 4. This means that all oxygen or nitrogen atoms form only bonds between network forming tetrahedrons resulting in an ideal three-dimensional network. On the opposite a glass with virtual composition like Mg_2SiO_4 gives a value of 0 what in turn states that not one of the oxygen atoms forms bridges between two silicon atoms, i.e. the structure consists of isolated SiO_4 tetrahedrons. The three-dimensional character of a glass network can be maintained down to an X value of 2.

3.3. Corrosion of the ceramic materials in 0.5 M H_2SO_4

The mass loss data and the thickness of the corrosion layers are given for the different ceramic materials in Figs. 7 and 8. At 60 °C a linear time dependence of the corrosion behaviour was observed for both the mass losses and the thickness of the corroded layers (Fig. 7). A linear change of the weight and corrosion depth takes place during the starting period of the corrosion at 90 °C (Fig. 8). The corrosion rate changes in a systematic man-

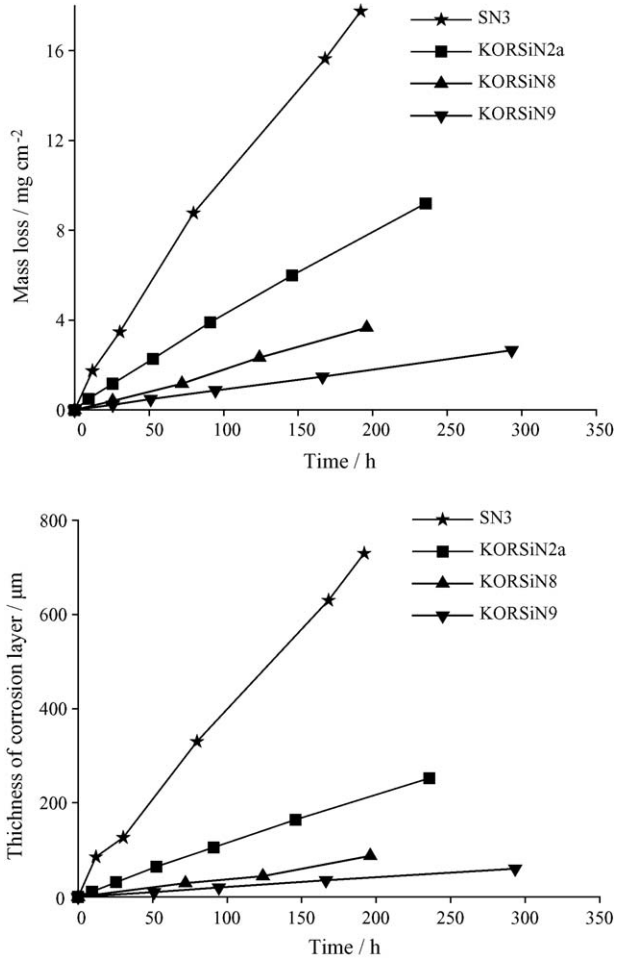

Fig. 7. Time-dependent mass loss data (a) and thicknesses of corrosion layer (b) for various ceramics containing different amounts of SiO_2 in the grain-boundary phase in 0.5 M sulphuric acid at 60 °C.

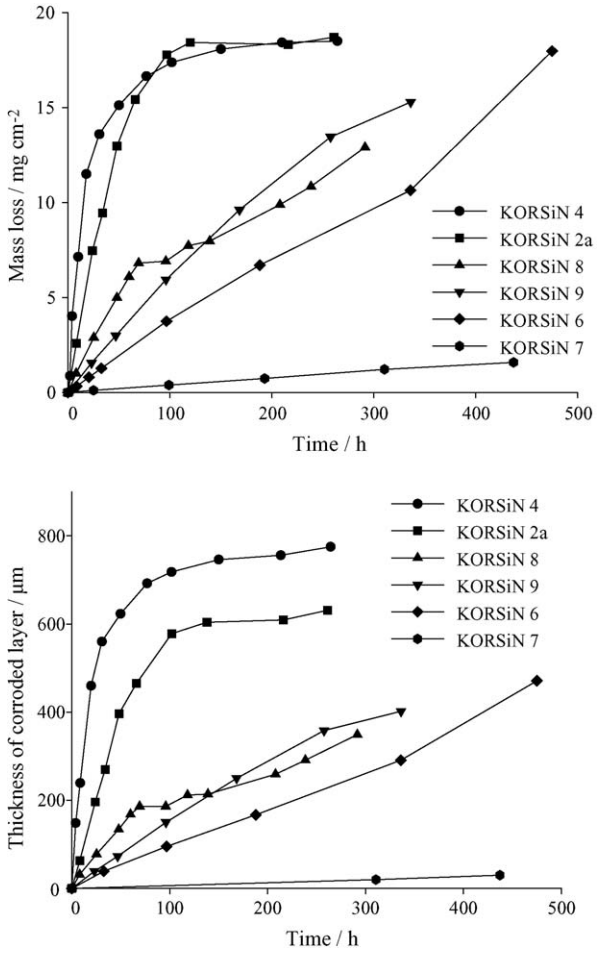

Fig. 8. Time-dependent mass loss data (a) and thicknesses of corrosion layers (b) for various ceramics containing different amounts of SiO_2 in the grain-boundary phase at 90 °C in 0.5 M sulfuric acid.

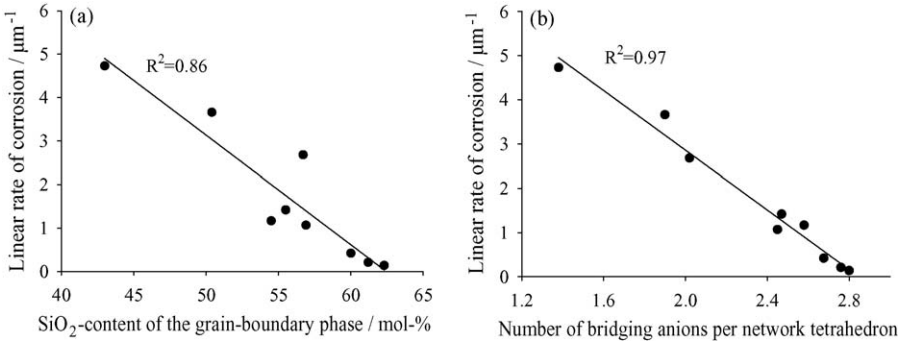

Fig. 9. Linear corrosion rates of KORSiN-and SN3-ceramics measured in 0.5 M 1 N H_2SO_4 at 60 °C in dependence of the SiO_2-content of the grain-boundary phase (a) and the number of bridging anions per network tetrahedron (b).

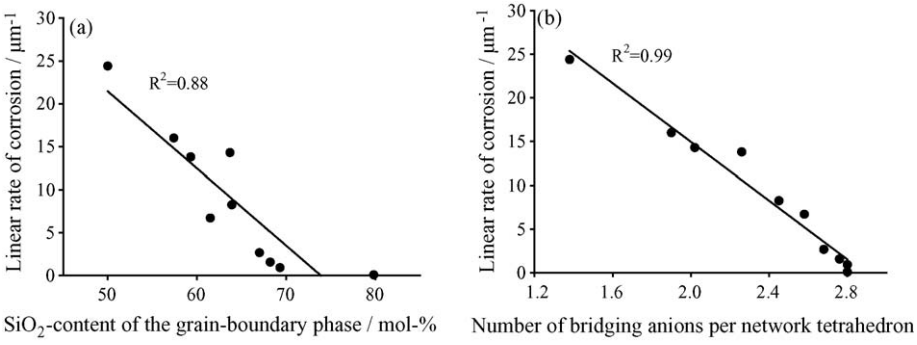

Fig. 10. Linear corrosion rates of KORSiN-and the SN0-and SN3-ceramics measured in 0.5 M 1 N H_2SO_4 at 90 °C in dependence of the SiO_2-content of the grain boundary phase (a) and the number of bridging anions per network tetrahedron (b).

ner with the composition. Materials with a low SiO_2 content in the grain boundary exhibit higher corrosion rates. Additionally, a strong reduction of the corrosion rate after 50 h corrosion time takes place in these materials during corrosion at 90 °C.

The linear reaction constants for the starting period are given in Table 4. A correlation of these data with the SiO_2 content and with number of bridging anions (X) per network forming cations is given in Fig. 9 for the 60 °C data and in Fig. 10 for the 90 °C data. The data show that the correlation is much better for the X-value than for the SiO_2 content. Similar relations were found recently for the corrosion constants of oxynitride glasses.[18] Fig. 11 shows that the determined linear corrosion rates of the investigated Si_3N_4 ceramics at 90 °C (time up to 50 h) correlate well with the corrosion rates of the oxynitride glasses having similar compositions. The small differences are probably caused by the uncertainties of the nitrogen content in the grain-boundary phases or could be related to the structure of the corrosion layer. The structure of the corrosion layer is also the reason for the retardation of the corrosion at longer corrosion times. The details of these processes will be discussed in part II of this series of papers.

Table 4
Linear corrosion rates of the Si_3N_4-ceramics in 0.5 MO_4 at 60 °C and 90 °C

Ceramic	X	Linear corrosion rate at	
		60 °C (k_h/µm h^{-1})	90 °C (k_h/µm h^{-1})
KORSiN 1	2.02	2.68	14.3
KORSiN 2a	2.45	1.07	8.3
KORSiN 4	1.38	4.73	24.4
KORSiN 5	2.57	1.17	6.7
KORSiN 6	2.80	0.14	0.9
KORSiN 8	2.68	0.42	2.7
KORSiN 9	2.76	0.21	1.6
KORSiN 7	2.80		0.07
SN3	1.90	3.66	16.0
SN0	2.26		13.8

X, number of bridging anions per network forming tetrahedron.

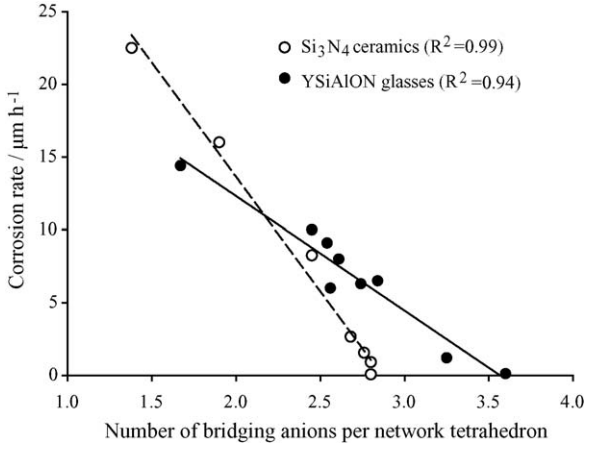

Fig. 11. Correlation of the linear corrosion rates of Y_2O_3/Al_2O_3-oxynitride glasses and of Si_3N_4 ceramics with Y_2O_3/Al_2O_3 containing grain boundaries.

4. Summary

The composition of the grain-boundary phase of Si_3N_4 ceramics is essential to the corrosion behaviour. The composition correlates with the amount of the starting sintering additives Y_2O_3 and Al_2O_3 but changes strongly during sintering due to the incorporation of Al and O into the Si_3N_4 lattice and the formation of $Si_{6-z}Al_zN_{8-z}O_z$.

The composition of the grain boundary can be calculated based on the amount of Al and O incorporated into the Si_3N_4 lattice determined by X-ray diffraction and by the total oxygen content of the material. It was not possible to distinguish by hot-gas extraction methods the oxygen in the grain-boundary phase and in the grains.

The corrosion resistance of the Si_3N_4 ceramics can be directly correlated with the composition and structure of the grain-boundary phase. The corrosion resistance in acids is the highest for materials with grain-boundary phases consisting of strongly linked networks.

References

1. Petzow, G. and Herrmann, M., Silicon nitride ceramics. *Structure and Bonding*, *Vol 102*. Springer Verlag, Berlin, Heidelberg, 2002, 47–167.
2. Schilm, J., Herrmann, M. and Michael, G., *J. Eur. Ceram. Soc.*, 2003, **23**, 577–584.
3. Seipel, B. and Nickel, K. G., *J. Eur. Ceram. Soc.*, 2003, **23**, 595–602.
4. Schilm, J., Korrosionsverhalten von Siliciumnitridkeramiken in Säuren, Promotion IKTS/TU BAF (2004).
5. Herrmann, M. and Goeb, O., Colour of gas-pressure-sintered silicon nitride ceramics. Part I and II. *J. Eur. Ceram. Soc.*, 2001, **21**, 303–314, 461–469.
6. Riedel, G., Bestgen, H., Herrman, M., Influence of sintering additives with differing proportions of Y_2O_3/Al_2O_3 on the sintering and materials properties of Si_3N_4-ceramics, cfi/Ber. DKG, 1998, **75**(10), 30–34; Riedel, G., Bestgen, H., Herrman, M., Correlation between structure and properties of Si_3N_4 materials with Y_2O_3/Al_2O_3 sintering additives, cfi/Ber. DKG, 1999 **76**(1–2), 24–27.
7. Shibata, N., Pennycook, S. J., Gosnell, T. R., Painter, G. S., Shelton, W. A. and Becher, P. F., Observation of rare earth segregation in silicon nitride ceramics at subnanometer dimensions. *Nature*, 2004, **428**, 730–773.
8. R. Satet, Einfluss der Grenzflächeneigenschaften auf die Gefügeausbildung und das mechanische Verhalten von Siliciumnitrid-Keramiken, Promotion, IKM Universität Karlsruhe (2003).
9. Rabe, T., Sontag, E., Kranz, G., Röhl, K. and Linke D, Analytische bestimmung der in siliciumnitrid vorliegenden phasen. In *Keramische Werkstoffe, Deutscher Wirtschaftsdienst*, ed. J. Kriegesmann. Köln, 1990. p. 6.1.
10. Schilm, J., Herrmann, M. and Michael, G., Leaching behaviour of silicon nitride materials in sulphuric acid containing KF. *J. Eur. Ceram. Soc.*, 2004, **24**, 2319–2327.
11. Kitayama, M., Hirao, K., Toriyama, M. and Kanzaki, S., Thermal conductivity of b-Si_3N_4: I, effects of various microstructural factors. *J. Am. Ceram. Soc.*, 1999, **82**, 3105–3117, 11.
12. Thomas, A. and Mueller, G., Alteration of oxygen content during powder conditioning and sintering of aluminum nitride ceramics. *CFI-Ceram. Forum Int.*, 1990, **67**(4), 146–149.
13. Ekström, T., Käll, P. O., Nygren, M. and Olson, P. O., Dense single-phase β-sialon ceramics by glass-encapsulated hot isostatic pressing. *J. Mater. Sci.*, 1989, **24**, 1853–1861, 5.
14. Lemercier, H., Rouxel, T., Fargeot, D., Besson, J.-L. and Piriou, B., Yttrium SiAlON glasses: structure and mechanical properties—elasticity and viscosity. *J. non-Cryst. Solids*, 1996, **201**, 128–145.
15. Jin, J., Sakka, S., Kozuka, H. and Yoko, T., Formation and chemical durability of Na–Si–O–N and Na–Al–Si–O–N oxynitride glasses. *J. Ceram. Soc. Jpn. Int. Ed.*, 1992, **100**, 841–846.
16. Risbud, S. H., Analysis of bulk amorphous oxnitride structures using the network theory of glasses. *Phys. Chem. Glasses*, 1981, **22**, 168–170, 6.
17. Hampshire, S., Oxynitride glasses, their properties and crystallisation—a review. *J. non-Cryst. Solids*, 2003, **316**, 64–73.
18. Schilm, J., Herrmann, M. and Michael, G., Corrosion of YSiAlON glasses in acidic and caustic media. *Silic. Ind.*, 2004, **69**(7–8), 317–324.
19. Scholze, H., *Glas Natur, Struktur und Eigenschaften*. Springer Verlag, Berlin, 1988.